Molecular weight effect on surface and bulk structure of poly(3-hexylthiophene) thin films

Matsumoto, Takuya ; Nishi, Keishirou ; Tamba, Shunsuke ; Kotera, Masaru ; Hongo, Chizuru ; Mori, Atsunori ; Nishino, Takashi

(Citation)
Polymer,119:76-82

(Issue Date)
2017-06-16

(Resource Type)
journal article

(Version)
Accepted Manuscript

(URL)
https://hdl.handle.net/20.500.14094/90004093

Molecular Weight Effect on Surface and Bulk Structure of Poly(3-hexylthiophene) Thin Films

*Takuya Matsumoto, Keishirou Nishi, Shunsuke Tamba, Masaru Kotera, Chizuru Hongo, Atsunori Mori, Takashi Nishino**

Department of Chemical Science and Engineering, Graduate School of Engineering, Kobe University Rokko, Nada, Kobe, 657-8501, Japan

Key Word

High head-to-tail regioregular poly(3-hexylthiophene); Grazing incidence X-ray diffraction; Thin film structure

ABSTRACT

Recently, the synthesis of P3HT with high head-to-tail regioregularity and the control of the molecular weight have been achieved. Herein, we evaluated the structure in thin films of various molecular weight P3HT (from M_w = 13k to 828k) prepared under diverse conditions through X-ray diffraction measurements. Higher molecular weight P3HT had the increase of "Face-on" structure in the thin films. From the structure of thin films prepared under other conditions, the main attribution was the speeds of sedimentation and inhabitation of the crystallization. Moreover, at the surface, the P3HT thin films with high molecular weight (M_w = 828k) emerged "Edge-on"-rich structure. With the larger distance from thin film surface, the structure gradually changed from "Edge-on" to "Face-on". These fundamental results would lead the suggestion in fabrication and performance of organic electronic devices.

Introduction

For several decade years, organic electronic devices have attracted much attentions in the view point of advantages on their flexibility, lightness and low-cost fabrication compared to inorganic material-based devices [1–4]. Especially, poly(3-hexylthiophene) (P3HT) shows a high hole carrier mobility and is applied as hole transport layers of various organic devices such as photovoltaic cells, fields-effect transistors, light-emitting diodes, thermoelectric transducers, memories and so on [5–8]. The low steric hindrance of the five-membered thiophene rings of P3HT leads the higher planarity of the main chain originated from π-π stacking and higher expansion of the conjugation system possesses relative to phenyl-based conjugated polymers. Therefore, the self-assembly of P3HT produces high crystallinity and high carrier mobility [9,10].

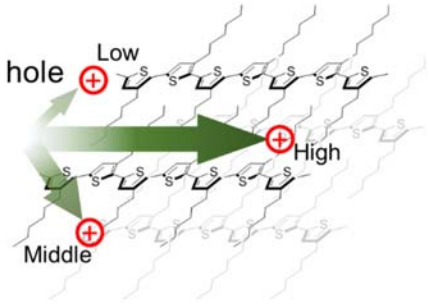

Figure 1. P3HT structure in crystallite and direction of hole mobilities

The carrier mobility of P3HT receives drastic effects on morphology and crystallite orientation in solid states. In particular, P3HT crystallites show anisotropic carrier mobility [9,11–14]. In the direction along the P3HT main chains, the crystallite shows the highest mobility. On the other hand, the mobility in the direction to π-π stacking of P3HT shows higher relative to that parallel to the side chains (Figure 1). Therefore, the control of crystallite orientation is a key factor for the electronic performance of various organic devices [9,11–14]. The crystallinity and crystallite

orientation have been considered to be variable according to regioregularity, molecular weight and end groups of P3HT, temperature and methods in the device fabrication, and affinity with surface of substrates. Recently, many researchers have discussed the effects of their factors [11–22]. However, in their discussion, they adopted P3HT with less molecular weight than 100,000 as high molecular weight P3HT, then they assumed that the structure at the surface is the same as that at bulk. The control of P3HT structure is highly controversial for their prominent performance in the organic devices.

Herein, we evaluated and compared the structure of P3HT thin films with various molecular weight (from 13k to 828k) in the bulk and at the surface. The P3HT in this research had high molecular weight as well as high head-to-tail regioregularity (>95%). We prepared thin films under various conditions such as molecular weights, solvents, temperature, rotational speeds in spin-casting and surface properties of substrates, and their effects on the structure of P3HT were investigated using small angle incidence / grazing incidence X-ray diffraction..

Experimental Section

Materials. All P3HT were synthesized with nickel catalysts according to our previous report [23]. All the reagents were obtained from commercial sources and used without further purification. ^{1}H (400 MHz) NMR spectra were recorded on JEOL ECZ400. ^{1}H NMR spectra were obtained with tetramethylsilane (TMS) as an internal standard in $CDCl_3$ at room temperature (Figure S1 in the Supplementary Data). Gel permeation chromatography (GPC) was carried out on JASCO LC-2000 Plus with UV-vis detector (at 254 nm) using Shodex GPC KF-404HQ and KF-402HQ using chloroform as an eluent after calibration with 6 polystyrene standards.

Preparation of hydrophilic and hydrophobic silicon wafer substrates. Hydrophilic silicon wafers were prepared in a piranha solution (sulfuric acid (H_2SO_4) / hydrogen peroxide (H_2O_2) = 3 : 1). After immersing in piranha solution for 15-20 min. at room temperature, the substrates were rinsed with deionized water and dried.

The hydrophobic substrates were prepared with silane coupling treatment to piranha-treated silicon wafers. The piranha-treated silicon wafers were immersed in 1-propanol and water (9 : 1) solution containing 3 wt% dodecyltriethoxysilane for 3 hours. After immersion, the substrates were washed with 1-propanol and dried at 100 °C for 1 h.

The surfaces of the modified silicon wafers were characterized with XPS (8 kV, 30 mA and pressure 5×10^{-6} Torr) and contact angles of water. The characterization data of both substrates were shown in Figure S2 in the Supplementary Data

Preparation of P3HT thin films. On the silicon wafer substrates, 650 μL chloroform or chlorobenzene solution containing 0.3 wt% P3HT at 50 °C was dropped on SPIN COATER IMC-

7094. The standard condition of spin-casting was 800 rpm for 5 sec and 3000 rpm for 1 min. Only when the rotational speed in spin-casting was compared, the condition was 500 rpm for 5 sec and various rotating speeds (500, 1000, 2000, 3000, 4000 and 5000 rpm) for 1 min. The cast thin films were prepared by casting 0.3 wt% P3HT solution, then dried at room temperature for 24 h.

Measurement of thickness of P3HT thin films. The thickness of P3HT thin films were measured by the X-ray reflection methods or the AFM. In the X-ray reflectivity carried on RIGAKU X-ray Diffractometer SmartLab, the power were 40 kV and 30 mA. The GXRR3 package was used for the curve fitting of the X-ray reflectance profiles (Figure S3 in the Supplementary Data) and then their thickness and roughness were evaluated. The thin films were scratched by sewing needles and P3HT layers were removed, then P3HT thickness was also estimated from the AFM height images by SII NanoTechnology, Navi E-sweep. The measurements were carried out in the dynamic force mode using silicon cantilevers. The surface roughness of the thin films was estimated from the AFM images. The roughness was presented by the root-mean-square (RMS) values using the equation (1):

$$\mathrm{RMS(nm)} = \sqrt{\frac{1}{X_{max}Y_{max}} \int_0^{Y_{max}} \int_0^{X_{max}} \{F(X,Y) - Z_0\}^2 dXdY} \qquad (1)$$

where X_{max}, Y_{max} are 20 μm, F(X,Y) is height at the pixel (X,Y) and Z_0 is the average of the height.

Measurement of X-ray diffraction. For the investigation of structure beneath the surface of thin films, X-ray diffraction was measured in the grazing incidence angels of X-ray beams (CuKα, λ = 1.5418 Å). The diffraction from the bulk structure in the thin films is observed in the measurement of small incidence angle X-ray diffraction with a little larger incidence angle than the critical angle (α_c). The total reflection of X-ray beams occurs below the critical angle (α_c). With the lower

incidence angles than α_c, the evanescent wave is observed and the structure within several nanometers from the surface is investigated. In contrast, with a little larger incident angles, the diffraction from the bulk structure is observed. In this work, we measured X-ray diffraction at the incidence angles 0.20° or below α_c. This 0.20° was an angle between the critical angles of P3HT (0.16°) and silicon wafer (0.23°). Therefore, the diffraction originated from silicon wafer substrates was inhibited.

For the investigation of the crystallite orientation in P3HT thin films on the silicon wafer substrates, the X-ray diffractions were detected by the scintillation counter with two different geometry; one was scanned in the direction perpendicular to the sample surface and the other was in the parallel direction. The former is called "Out-of-plane" measurement and the later is "In-plane" measurement. In the "Out-of-plane" geometry, the lattice planes nearly parallel to the surface of thin films are detected. In contrast, in the "In-plane" geometry, the lattice planes nearly perpendicular to the surface are observed.

The penetration depth of X-ray beam from the surface was around 1.7 μm at α = 0.20°. (see the section "Penetration depth of X-ray beam" and Figure S4 in the Supplementary Data)

Results and Discussion

Characterization. All the P3HT were synthesized through the deprotonative polymerization with the Knochel-Hauser base (TMPMgCl·LiCl) catalyzed by CpNiCl(SIPr) in the reported method [23–25]. The molecular weight and molecular weight distribution are shown in Table 1. The distribution of several P3HT samples were larger relatively. However, there was no effect of the PDI on the following investigation in this work. The obtained P3HT had high head-tail regioregularity (>95%) from their ^{1}H NMR spectra (Figure S1 in Supplementary Data). From the height images of AFM, the thickness and roughness of P3HT thin films are shown in Table 1. All the spin-coated films had similar thickness and high smoothness. The film prepared by casting method had larger thickness than 100 μm. In only the X-ray reflectivity profile of the thin film of lowest molecular weight P3HT (M_w =13k), the fringe was observed (Figure S2 in Supplementary Data): the thickness of 34 nm was almost equal to that estimated by the height image of AFM.

Table 1. Molecular weight of P3HT samples.

P3HT film	Weight-average Molecular weight M_w	Number-average Molecular weight M_n	PDI (M_w / M_n)	Thickness[a]	RMS[a]
				nm	nm
13k	13,400	10,700	1.26	30, 34[b]	1.09
128k	128,000	23,900	5.37	40	1.44
212k	212,000	103,000	2.06	50	2.50
346k	346,000	175,000	1.98	40	5.38
828k	828,000	264,000	3.14	70	2.35

[a] Measured by AFM height images. [b] Calculated by X-ray reflectivity measurements.

Effect of molecular weight. We prepared thin films of P3HT with various molecular weight (M_w = 13k, 128k, 214k, 346k, 828k) on the hydrophilic silicon wafer substrates. Their structures were investigated by the small angle incidence / grazing incidence X-ray diffraction. In all the profiles of P3HT thin films, the peaks originated from P3HT crystallite were observed. Their peaks could be indexed with the reported crystal structure of P3HT [10]. For comparison, the powder diffraction of P3HT annealed at 100 °C for 1 hour was measured. The 100 and 020 reflections were observed at 2θ = 5°, 23° respectively (Figure S7 in the Supplementary Data). The intensity ratio from 100 to 020 diffraction peak (I_{100}/I_{020}) of 3.0 was represented for the non-oriented ones.

The X-ray diffraction profiles of P3HT films with various molecular weights through "Out-of-plane" and "In-plane" geometries are shown in Figure 2a and 2b, respectively. Then, the intensity ratio of 100 to 020 diffraction peak (I_{100}/I_{020}) in the each profile is shown in Figure 2c. With increasing the molecular weight, the ratios of I_{100}/I_{020} in the "Out-of-plane" geometry decreased obviously. In contrast, the ratios of I_{100}/I_{020} in the "In-plane" increased. In the low molecular weight P3HT ($M_w \leqq$ 346k), the I_{100}/I_{020} were larger in the "Out-of-plane" geometry and smaller in the "In-plane" than that of the powder sample. This means that the P3HT with lower molecular weight had "Edge-on"-rich structures, as previously reported [9]. As the increase of the molecular weights, the structures in thin films transformed from "Edge-on" to "Face-on" gradually. In the thin film of P3HT (M_w = 828k), the ratio of "Edge-on" and "Face-on" structures was inverted.

Sirringhaus *et. al.* have reported the effect of molecular weight of P3HT on the thin film structures [9]. In their report, the main structures of P3HT with low molecular weight (M_w = 11k, 28k) and high head-to-tail regioregularity (91%, 95%) were "Edge-on", whereas those with high molecular weight (M_w = 126k, 175k) and low head-to-tail regioregularity (70%, 81%) were "Face-on". This report was in contrast with our measurements for P3HT (128k and 214k), where both

showed “Edge-on”-rich structure. In order to investigate the dissimilarity between Sirringhaus’ work and ours, besides the difference of the head-to-tail ratios, several factors were investigated. Especially, in the following discussion, we focused on the “Face-on”-rich structure of the thin film of P3HT (M_w = 828k).

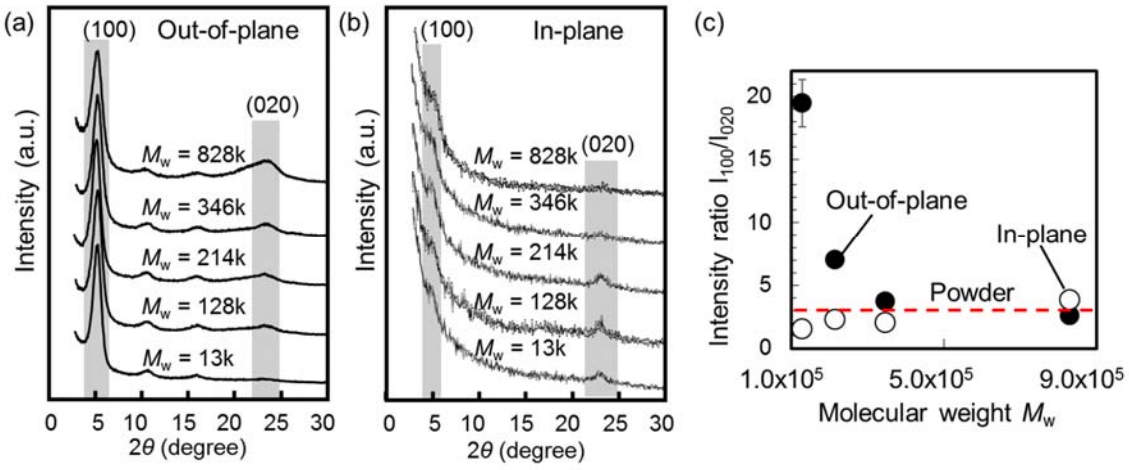

Figure 2. (a) "Out-of-plane" and (b) "In-plane" small angle incidence X-ray diffraction profiles of P3HT thin films with various molecular weights spin-coated on piranha treated silicon wafers. (c) Relationship between intensity ratio of 100/020 and molecular weight M_w of P3HT thin films.

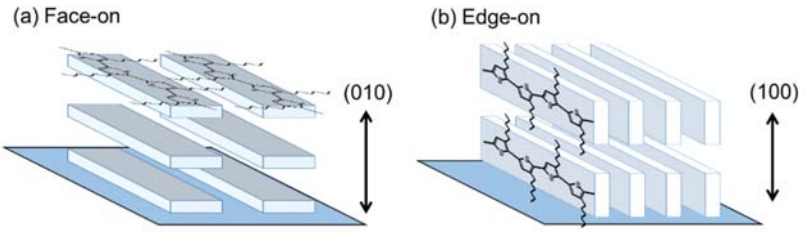

Figure 3. Schematic Models of (a) "Face-on" and (b) "Edge-on" configuration for P3HT thin films on silicon wafers.

Effect of solvents and temperature. P3HT (M_w = 828k) thin films were prepared by spin-coating chloroform and *o*-dichlorobenzene solution on the piranha treated silicon wafers at 25 °C and 55 °C, respectively. In Figure 4a and 4b, the X-ray diffraction profiles are shown in the "Out-of-plane" and "In-plane" geometries. In the "Out-of-plane" profiles, the I_{100}/I_{020} ratio in the thin film prepared from *o*-dichlorobenzene solution was larger than that from chloroform, while, in the "In-

plane" measurements, the I_{100}/I_{020} ratio of thin film prepared from *o*-dichlorobenzene decreased relative to that from chloroform. These indicates that the P3HT thin film with high molecular weight possessed "Edge-on"-rich structure even prepared from *o*-dichlorobenzene solution instead of chloroform solution.

Figure 4c and 4d show X-ray diffraction profiles of P3HT (M_w = 828k) thin films prepared from chloroform solution at 25 °C and 55 °C. The thin films prepared at 55 °C possessed the larger I_{100}/I_{020} ratio in the "Out-of-plane" measurements and smaller ratio in the "In-plane" than those prepared at 25 °C. In the structure of thin films prepared at 55 °C, the ratio of "Face-on" structure was increased relatively.

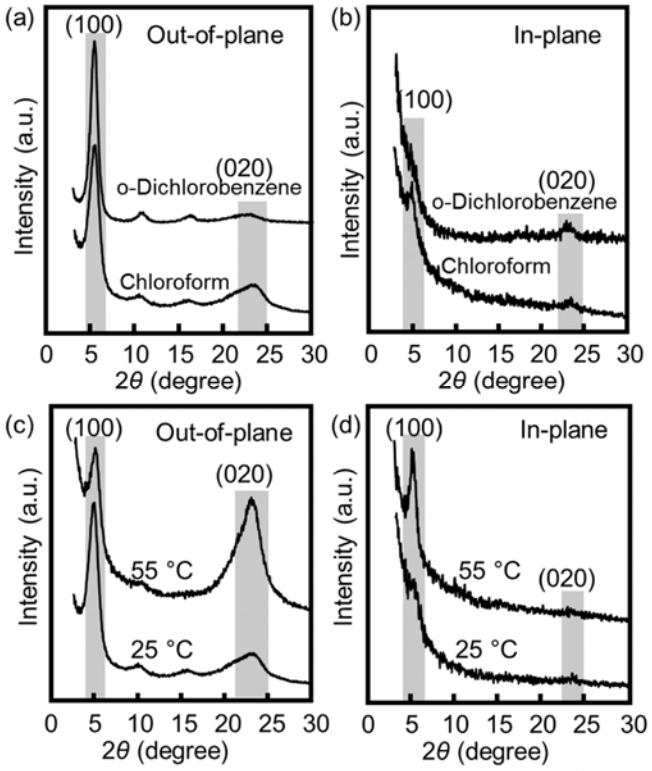

Figure 4. (a,c) "Out-of-plane" and (b,d) "In-plane" small angle incidence X-ray diffraction profiles of P3HT (M_w = 828k) thin films (a,b) with various solvents and (c,d) at various temperature spin-coated on piranha treated silicon wafers.

Effect of rotational speed in spin-casting. P3HT (M_w = 828k) thin films were prepared in spin-coating with various rotational speeds from 500 rpm to 5000 rpm. The thickness of thin films prepared with various rotational speeds is shown in Table S3 in the Supplementary Data and the X-ray profiles are shown in Figure 5a and 5b. As the rotation speed increased, the I_{100}/I_{020} ratios in the "Out-of-plane" measurement were decreased and the ratios in the "In-plane" were decreased (Figure 5c). These results mean that the structure of thin films changed from "Edge-on"-rich to "Face-on"-rich with the increase of rotational speed. In addition, the thin film prepared in the cast method showed the 020 diffraction peak only in the "In-plane" measurement (Figure 6). This reveals that the P3HT as-cast films possessed only the "Edge-on" structure.

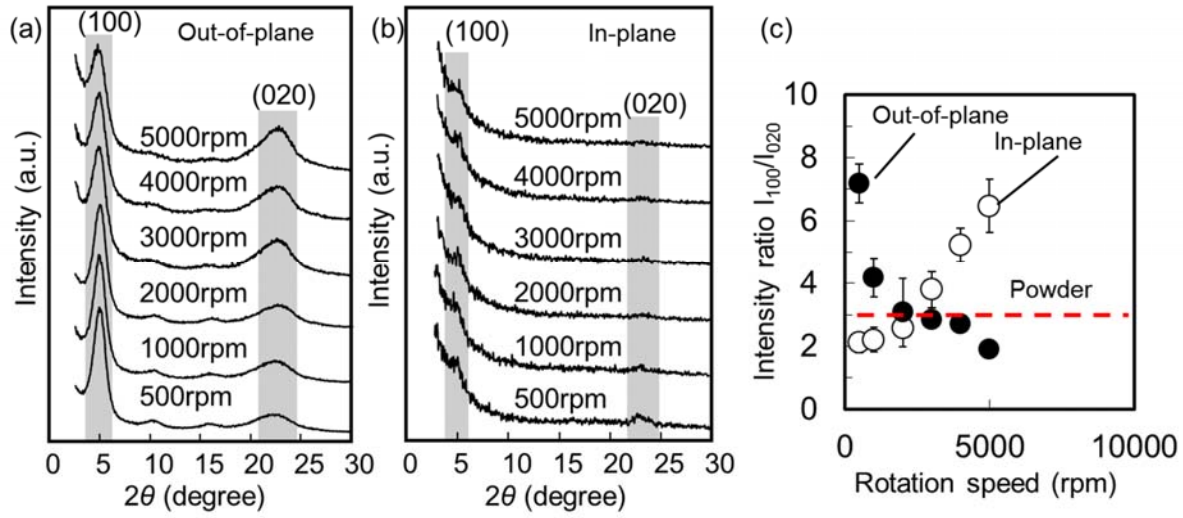

Figure 5. (a) "Out-of-plane" and (b) "In-plane" small angle incidence X-ray diffraction profiles of P3HT (M_w = 828k) spin-coated on piranha treated silicon wafers with different rotation speed. (c) Relationship between the 100/020 intensity ratio and the rotation speed of spin-coating.

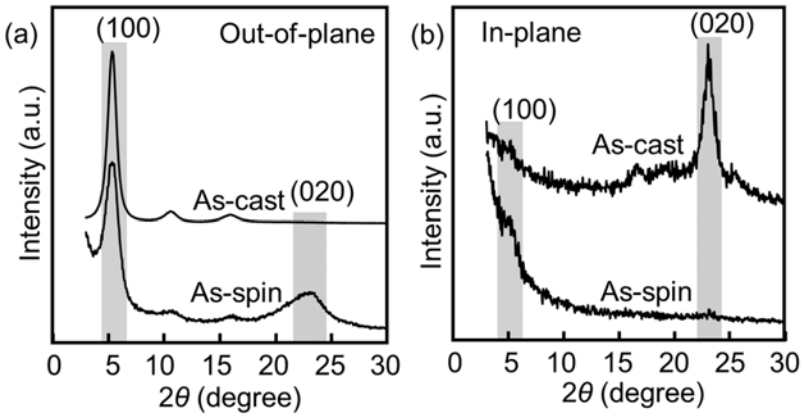

Figure 6. (a) "Out-of-plane" and (b) "In-plane" small angle incidence X-ray diffraction of P3HT (M_w = 828k) thin film with different fabrication method.

Factors of structure control of P3HT thin films. As described above, we investigated the structure of P3HT thin films prepared under various conditions such as molecular weight, solvents, temperature and rotational speed. It is clarified that spin-coating of P3HT with high molecular weight, from high volatile solvents, at high temperature or with high speed rotational speed led "Face-on"-rich structure. Under these conditions, the thin films were formed rapidly. The viscosity of chloroform solution of P3HT with high molecular weight was much higher than that with low molecular weight. This high viscosity would result in the delay of sedimentation and crystallization on the silicon wafer substrates. Moreover, the slow evaporation in the cast method led to the "Edge-on" structure. Thus, it is suggested that the "Face-on" structure would be a kinetically preferable state and "Edge-on" would be a thermodynamically one.

Surface structure of P3HT thin films. In the above discussion, we have investigated the bulk structure of thin films from the result of the small angle incidence X-ray diffraction, where the incidence angles were 0.20°, being larger than the critical angles α_c (0.16°). The penetration depth

of the X-ray beams with various incidence angles is shown in Figure S4 in the Supplementary Data. In the X-ray diffraction measurement with the grazing incidence angles below α_c, we can investigate the structure within about 10 nm from the top surface of thin films.

Figure 7a and 7b show the X-ray diffraction profiles of P3HT thin films (M_w = 13k and 828k) in the "Out-of-plane" measurement with various incidence angles. P3HT thin film (M_w = 13k) at the surface showed the "Edge-on"-rich structure similar to the bulk. The I_{100}/I_{020} ratios were larger than 20 at all the incident angles. In contrast, the I_{100}/I_{020} ratio of P3HT thin film (M_w = 828k) decreased with the lower incidence angles of X-ray beams as shown in Figure7c. These results mean that the thin film possessed the more "Edge-on"-rich structure at the nearer surface. Accordingly, P3HT thin film (M_w = 828k) possesses heterogeneous structure in the thickness direction of the same film, *that is*, "Face-on"-rich was observed in the bulk and "Edge-on"-rich was at the surface.

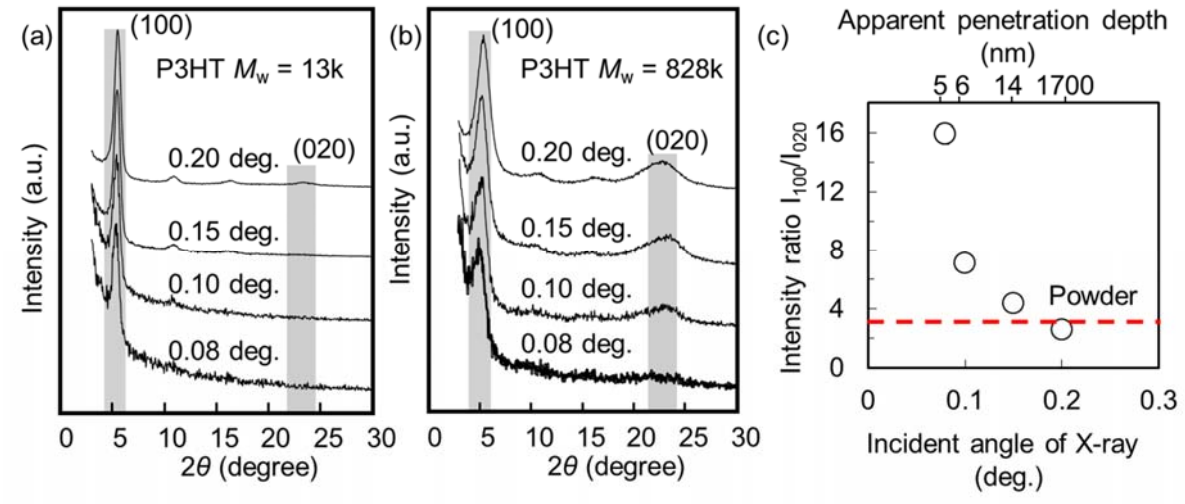

Figure 7. "Out-of-plane" X-ray diffraction profiles of P3HT (M_w = (a) 13k, (b) 828k) thin films with different incident angles, spin-coated on piranha treated silicon wafers. (c) Relationship between intensity ratio of 100/020 in P3HT thin films (M_w = 828k) and incident angles of X-ray

beams. The intensities of 100/020 in P3HT thin films (M_w = 13k) were unavailable because of the exceptionally low intensities of 100 peaks.

Effect of surface treatment of silicon wafer substrates. In Figure S2 in the Supplementary Data, we show the XPS profiles and water droplets on the piranha treated and silane coupling treated silicon wafers, respectively. The silane coupling treatment, performed by immersing piranha treated silicon wafers into dodecyltriethoxysilane solution, showed high water repellency.

We first investigated the bulk structure of P3HT thin films with the small angle incidence X-ray diffraction ($>\alpha_c$). The X-ray diffraction profiles of P3HT thin films with various molecular weight on the silane coupling treated silicon wafers is shown in Figure 8. As observed in the thin films on the piranha treated silicon wafers, the I_{100}/I_{020} ratio of P3HT thin films in the "Out-of-plane" measurement decreased and those in the "In-plane" increased with higher molecular weight of P3HT. These results suggested that the ratio of "Edge-on" structure to "Face-on" decreased for higher molecular weight P3HT. However, all the P3HT thin films including high molecular weight P3HT (M_w = 828k) had "Edge-on"-rich structure, which was in contrast to the results in Figure 2. It is suspected that "Edge-on" structure at the interface of the silicon wafer might be formed though the interaction between alkyl chains of P3HT and those on the silicon wafers, then epitaxial crystal grown to the thickness direction [26].

For the investigation of the surface structures of P3HT thin films (M_w = 13k and 828k), we adapted grazing incidence X-ray diffraction measurements. In the profiles of both thin films, 100 diffraction peaks or shoulders, but not 020 diffraction, were observed at the grazing incidence angles 0.08° below the critical angle (Figure 9). Relative to P3HT thin films on the silane coupling treated substrates, the 100 diffraction peaks of thin films on the piraniha treated substrates were

sharpened distinctly in the grazing incidence X-ray diffraction measurements (Figure S8 and S9 in the Supplementary Data). This means that the crystallinity at the surface of thin films on the hydrophobic substrates could be decreased compared to that on hydrophilic ones.

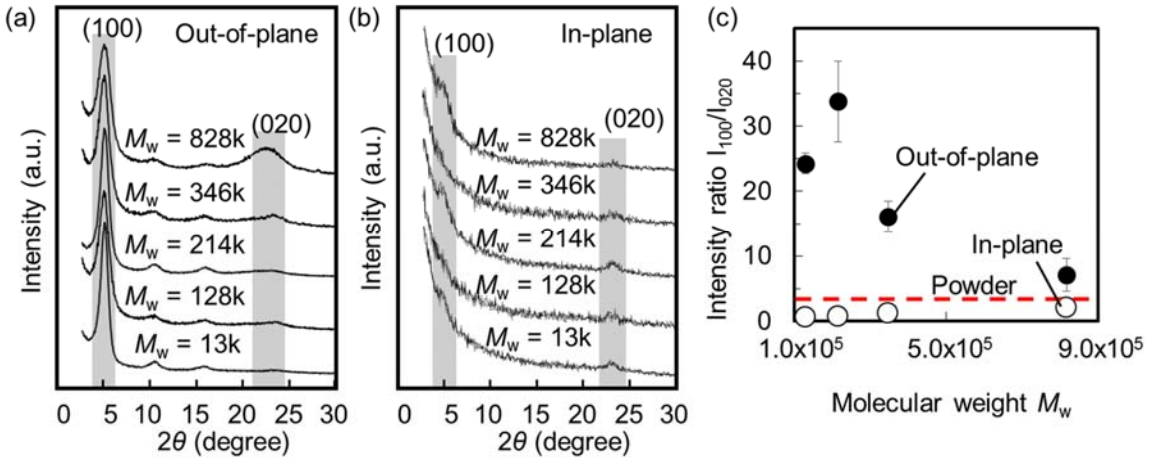

Figure 8. (a) "Out-of-plane" and (b) "In-plane" X-ray diffraction profiles of P3HT thin films with various molecular weight, spin-coated on silane coupling treated silicon wafers. (c) Relationship between intensity ratio of 100/020 and molecular weight M_w of P3HT thin film.

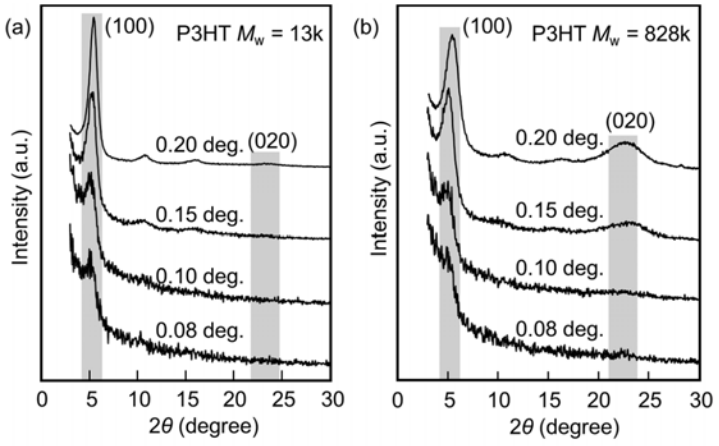

Figure 9. "Out-of-plane" X-ray diffraction profiles of P3HT (M_w = (a) 13k, (b) 828k) thin films with different incident angle, spin-coated on silane coupling treated silicon wafer.

CONCLUSIONS

We investigated the thin film structure of P3HT with various molecular weight from M_w = 13k to 828k and high head-to-tail regioregularity (>95%) using small angle and grazing incidence X-ray diffraction. From the results of small angle incidence X-ray diffraction, the structures in thin films were transformed from the "Edge-on" to "Face-on" with the increase of molecular weight. In the thin film of high molecular weight P3HT, the bulk structure was "Face-on"-rich, whereas the surface was "Edge-on"-rich. Even in the same thin films, the structure was gradually changed from the bulk to the surface. Moreover, the surface properties of substrates affected on the thin film structure at the surface. These results give the valuable insight on the epitaxial crystal growing in the fabrication of electronic devices and the charge transport across layers of their devices.

ASSOCIATED CONTENT

Supplementary Data.

This material is available free of charge via the Internet at http://

AUTHOR INFORMATION

Corresponding Author

*(T.N.) E-mail: tnishino@kobe-u.ac.jp

Funding Sources

This work was partially supported by a Grant-in-Aid for Scientific Research on Innovative Areas "New Polymeric Materials Based on Element-Blocks (No.2401)" (24102009) of The Ministry of Education, Culture, Sports, Science, and Technology, Japan.

Notes

The authors declare no competing financial interest.

Acknowledgements

The synchrotron radiation experiments were performed at the BL15XU, BL24XU of SPring-8 with the approval of the National Institute for Materials Science (NIMS) (Proposal No. 2011B3255, 2012A4803, 2012B4803). The 2DGIXRD is shown in Figure S10 in Supplementary Data

REFERENCES

[1] K.M. Coakley, and Michael D. McGehee, Conjugated Polymer Photovoltaic Cells, *Chem. Mater.* 16 (2004) 4533–4542. doi:10.1021/cm049654n.

[2] Y. Shirota, Organic materials for electronic and optoelectronic devices, *J. Mater. Chem.* 10 (2000) 1–25. doi:10.1039/A908130E.

[3] S.R. Forrest, The path to ubiquitous and low-cost organic electronic appliances on plastic, *Nature*. 428 (2004) 911–918. doi:10.1038/nature02498.

[4] P. Peumans, A. Yakimov, S.R. Forrest, Small molecular weight organic thin-film photodetectors and solar cells, *J. Appl. Phys.* 93 (2003) 3693–3723. doi:10.1063/1.1534621.

[5] Y. Li, Molecular Design of Photovoltaic Materials for Polymer Solar Cells: Toward Suitable Electronic Energy Levels and Broad Absorption, *Acc. Chem. Res.* 45 (2012) 723–733. doi:10.1021/ar2002446.

[6] M.T. Dang, L. Hirsch, G. Wantz, J.D. Wuest, Controlling the Morphology and Performance of Bulk Heterojunctions in Solar Cells. Lessons Learned from the Benchmark Poly(3-hexylthiophene):[6,6]-Phenyl-C61-butyric Acid Methyl Ester System, *Chem. Rev.* 113 (2013) 3734–3765. doi:10.1021/cr300005u.

[7] C.D. Dimitrakopoulos, P.R.L. Malenfant, Organic Thin Film Transistors for Large Area Electronics, *Adv. Mater.* 14 (2002) 99–117. doi:10.1002/1521-4095(20020116)14:2<99::AID-ADMA99>3.0.CO;2-9.

[8] R.A. Segalman, B. McCulloch, S. Kirmayer, J.J. Urban, Block Copolymers for Organic Optoelectronics, *Macromolecules.* 42 (2009) 9205–9216. doi:10.1021/ma901350w.

[9] H. Sirringhaus, P.J. Brown, R.H. Friend, M.M. Nielsen, K. Bechgaard, B.M.W. Langeveld-Voss, A.J.H. Spiering, R.A.J. Janssen, E.W. Meijer, P. Herwig, D.M. de Leeuw, Two-dimensional charge transport in self-organized, high-mobility conjugated polymers, *Nature*. 401 (1999) 685–688. doi:10.1038/44359.

[10] T.J. Prosa, M.J. Winokur, J. Moulton, P. Smith, A.J. Heeger, X-ray structural studies of poly(3-alkylthiophenes): an example of an inverse comb, *Macromolecules*. 25 (1992) 4364–4372. doi:10.1021/ma00043a019.

[11] A. Salleo, Charge transport in polymeric transistors, *Mater. Today.* 10 (2007) 38–45. doi: 10.1016/S1369-7021(07)70018-4.

[12] R. Joseph Kline, M.D. McGehee, M.F. Toney, Highly oriented crystals at the buried interface in polythiophene thin-film transistors, *Nat Mater.* 5 (2006) 222–228. doi:10.1038/nmat1590.

[13] Dean M. DeLongchamp, Brandon M. Vogel, Youngsuk Jung, Marc C. Gurau, Curt A. Richter, Oleg A. Kirillov, Jan Obrzut, Daniel A. Fischer, Sharadha Sambasivan, Lee J. Richter, and Eric K. Lin, Variations in Semiconducting Polymer Microstructure and Hole Mobility with Spin-Coating Speed, *Chem. Mater.* 17 (2005) 5610–5612. doi:10.1021/cm0513637.

[14] D.H. Kim, J.T. Han, Y.D. Park, Y. Jang, J.H. Cho, M. Hwang, K. Cho, Single-Crystal Polythiophene Microwires Grown by Self-Assembly, *Adv. Mater.* 18 (2006) 719–723. doi:10.1002/adma.200502442.

[15] B. Meredig, A. Salleo, R. Gee, Ordering of Poly(3-hexylthiophene) Nanocrystallites on the Basis of Substrate Surface Energy, *ACS Nano.* 3 (2009) 2881–2886. doi:10.1021/nn800707z.

[16] R.J. Kline, M.D. McGehee, E.N. Kadnikova, J. Liu, J.M.J. Fréchet, Controlling the Field-Effect Mobility of Regioregular Polythiophene by Changing the Molecular Weight, *Adv. Mater.* 15 (2003) 1519–1522. doi:10.1002/adma.200305275.

[17] R. Joseph Kline, Michael D. McGehee, Ekaterina N. Kadnikova, Jinsong Liu, Jean M. J. Fréchet, and Michael F. Toney‖, Dependence of Regioregular Poly(3-hexylthiophene) Film Morphology and Field-Effect Mobility on Molecular Weight, *Macromolecules.* 38 (2005) 3312–3319. doi:10.1021/ma047415f.

[18] Achmad Zen, Marina Saphiannikova, Dieter Neher, Jörg Grenzer, Souren Grigorian, Ullrich Pietsch, Udom Asawapirom, Silvia Janietz, Ullrich Scherf, Ingo Lieberwirth, and Gerhard Wegner, Effect of Molecular Weight on the Structure and Crystallinity of Poly(3-hexylthiophene), *Macromolecules*. 39 (2006) 2162–2171. doi:10.1021/ma0521349.

[19] M. Brinkmann, P. Rannou, Molecular Weight Dependence of Chain Packing and Semicrystalline Structure in Oriented Films of Regioregular Poly(3-hexylthiophene) Revealed by High-Resolution Transmission Electron Microscopy, *Macromolecules*. 42 (2009) 1125–1130. doi:10.1021/ma8023415.

[20] J.-M. Verilhac, G. LeBlevennec, D. Djurado, F. Rieutord, M. Chouiki, J.-P. Travers, A. Pron, Effect of macromolecular parameters and processing conditions on supramolecular organisation, morphology and electrical transport properties in thin layers of regioregular poly(3-hexylthiophene), *Synth. Met.* 156 (2006) 815–823. doi:10.1016/j.synthmet.2006.04.012.

[21] A. Zen, J. Pflaum, S. Hirschmann, W. Zhuang, F. Jaiser, U. Asawapirom, J.P. Rabe, U. Scherf, D. Neher, Effect of Molecular Weight and Annealing of Poly(3-hexylthiophene)s on the Performance of Organic Field-Effect Transistors, *Adv. Funct. Mater.* 14 (2004) 757–764. doi:10.1002/adfm.200400017.

[22] R.J. Kline, D.M. DeLongchamp, D.A. Fischer, E.K. Lin, L.J. Richter, M.L. Chabinyc, M.F. Toney, M. Heeney, I. McCulloch, Critical Role of Side-Chain Attachment Density on the Order and Device Performance of Polythiophenes, *Macromolecules* 40 (2007) 7960–7965. doi:10.1021/ma0709001.

[23] S. Tamba, K. Fuji, H. Meguro, S. Okamoto, T. Tendo, R. Komobuchi, A. Sugie, T. Nishino, A. Mori, Synthesis of High-molecular-weight Head-to-tail-type Poly(3-substituted-thiophene)s by Cross-coupling Polycondensation with [CpNiCl(NHC)] as a Catalyst, *Chem. Lett.* 42 (2013) 281–283. doi:10.1246/cl.2013.281.

[24] K. Fujita, Y. Sumino, K. Ide, S. Tamba, K. Shono, J. Shen, T. Nishino, A. Mori, T. Yasuda, Synthesis of Poly(3-substituted thiophene)s of Remarkably High Solubility in Hydrocarbon via Nickel-Catalyzed Deprotonative Cross-Coupling Polycondensation, *Macromolecules*. 49 (2016) 1259–1269. doi:10.1021/acs.macromol.5b02524.

[25] A. Krasovskiy, V. Krasovskaya, P. Knochel, Mixed Mg/Li Amides of the Type $R_2NMgCl{\cdot}LiCl$ as Highly Efficient Bases for the Regioselective Generation of Functionalized Aryl and Heteroaryl Magnesium Compounds, *Angew. Chemie Int. Ed.* 45 (2006) 2958–2961. doi:10.1002/anie.200504024.

[26] S.-J. Kang, Y.-S. Kim, W.B. Kim, D.-Y. Kim, Y.-Y. Noh, Conjugated Polymer Chain and Crystallite Orientation Induced by Vertically Aligned Carbon Nanotube Arrays, *ACS Appl. Mater. Interfaces.* 5 (2013) 9043–9050. doi:10.1021/am402264m.

TOC

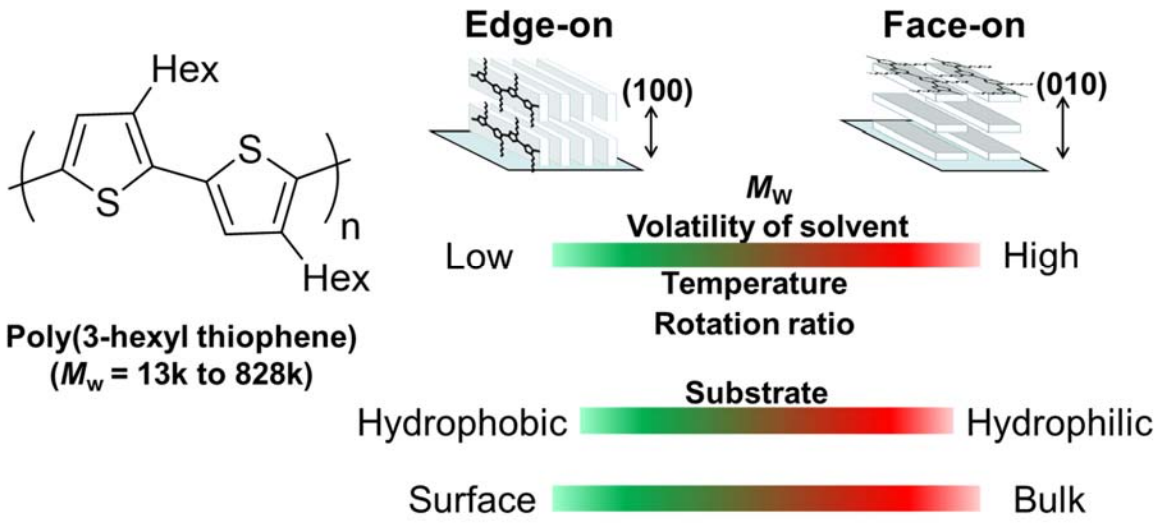
Hex
S
S
n
Hex
Poly(3-hexyl thiophene)
(M_w = 13k to 828k)
Edge-on
(100)
Face-on
(010)
M_w
Volatility of solvent
Low
High
Temperature
Rotation ratio
Substrate
Hydrophobic
Hydrophilic
Surface
Bulk